

Attenuation Correction of PET Images with Respiration-Averaged CT Images in PET/CT

Tinsu Pan, PhD¹; Osama Mawlawi, PhD¹; Sadek A. Nehmeh, PhD²; Yusuf E. Erdi, PhD²; Dershan Luo, PhD³; Hui H. Liu, PhD³; Richard Castillo, MS³; Radhe Mohan, PhD³; Zhongxing Liao, MD⁴; and H.A. Macapinlac, MD⁵

¹Department of Imaging Physics, The University of Texas M.D. Anderson Cancer Center, Houston, Texas; ²Department of Medical Physics, Memorial Sloan-Kettering Cancer Center, New York, New York; ³Department of Radiation Physics, The University of Texas M.D. Anderson Cancer Center, Houston, Texas; ⁴Department of Radiation Oncology, The University of Texas M.D. Anderson Cancer Center, Houston, Texas; and ⁵Department of Nuclear Medicine, The University of Texas M.D. Anderson Cancer Center, Houston, Texas

Attenuation correction (AC) of PET images with helical CT (HCT) in PET/CT matches only the spatial resolution of CT and PET, not the temporal resolution. We therefore proposed the use of respiration-averaged CT (ACT) to match the temporal resolution of CT and PET and evaluated the improvement of tumor quantification in PET images of the thorax with ACT. **Methods:** First, we examined 100 consecutive clinical PET/CT studies for the frequency and magnitude of misalignment at the diaphragm position between the HCT and the PET data. Patients were injected with 555–740 MBq of ¹⁸F-FDG and scanned 1 h after injection. The HCT data were acquired at the following settings: 120 kV, 300 mA, pitch of 1.35:1, collimation of 8×1.25 mm, and rotation cycle of 0.5 s. Patients were instructed to hold their breath at midexpiration during HCT of the thorax. The PET acquisition was 3 min per bed. Second, we retrospectively analyzed studies of 8 patients (1 with esophageal cancer and 7 with lung cancer). Each study included regular PET/CT followed by 4-dimensional (4D) CT for radiation treatment planning. We compared the results of AC of the PET data with HCT and ACT. There were 13 tumors in these 8 patients. The 4D CT data were acquired at the following settings: 120 kV, 50–150 mA, cine duration of 1 breathing cycle plus 1 s, collimation of 8×1.25 mm, and rotation cycle of 0.5 s. The acquisition was taken when the patient was in the free-breathing state. We averaged the 10 phases of the 4D CT data to obtain ACT for AC of the PET data. Both the ACT and the HCT data were used for AC of the same PET data. **Results:** There was a misalignment between the HCT and the PET data in 50 of 100 patient studies. In 34 studies, the misalignment was greater than 2 cm. In a comparison of HCT and ACT, 5 tumors had differences in standardized uptake values (SUV) between HCT- and ACT-attenuation-corrected PET of less than 20%, and 4 tumors had differences in SUV of more than 50%. The latter 4 tumors were found in the patient with esophageal cancer and in 2 of the patients with lung cancer. The PET data from these 3 patients had a misalignment of 2–4.5 cm relative to the HCT data. Breathing artifacts were significantly reduced by ACT. Seven of the 8 patients had a lower diaphragm position on HCT than on ACT, suggesting that

the patients tended to hold a deeper breath during HCT than during ACT. **Conclusion:** The high rate of misalignment suggested a potential mismatch between the HCT and the PET data with the limited-breath-hold CT protocol. In the comparison of HCT and ACT, significant differences (>50%) in SUV were attributable to different breathing states between HCT and PET. The PET data corrected by ACT did not show breathing artifacts, suggesting that ACT may be more accurate than HCT for AC of the PET data.

Key Words: attenuation correction; breathing artifacts; 4D CT; PET/CT

J Nucl Med 2005; 46:1481–1487

PET/CT can provide both anatomic information and functional information in a single imaging session as well as accurate registration of PET and CT data to improve the diagnosis of tumors (1–8). Additionally, high-performance and high-throughput multislice CT also has replaced transmission rod sources to obtain an attenuation map for the quantification of PET emission data (9–11). The scan time with transmission rod sources is several minutes for only 15 cm of coverage, but the scan time is reduced to only about 30 s for 100 cm of coverage with high-throughput multislice CT. A PET/CT scan thus typically takes less than 30 min instead of more than 1 h, as with a stand-alone PET scanner (12).

In a PET/CT scan, a helical CT (HCT) scan normally is performed before the PET scan to obtain a CT-based attenuation map for attenuation correction (AC) of the PET data and to provide anatomic information to improve the localization of tumors in PET images (12). Performing CT before PET allows the PET data to be reconstructed with AC before the patient leaves the scanner and ensures the integrity of data acquisition. To match the CT and the PET data, patients are asked during the HCT scan to either hold their breath at midexpiration or take a shallow breath. Misalignment of the HCT and the PET data has been reported with both techniques and may become an issue in imaging the

Received Mar. 17, 2005; revision accepted May 10, 2005.

For correspondence or reprints contact: Tinsu Pan, PhD, Department of Imaging Physics, Unit 56, The University of Texas M.D. Anderson Cancer Center, 1515 Holcombe Blvd., Houston, TX 77030.

E-mail: tpan@mdanderson.org

thorax because the breath-hold state in HCT is different from the free-breathing state in PET. The end results are a mismatch of tumor location between HCT and PET scans and inaccurate quantification of tumors in PET images (13–17).

We have examined the temporal resolution and the spatial resolution of CT and PET. CT images have a temporal resolution of less than 1 s and an in-plane spatial resolution of less than 1 mm, whereas PET images have a temporal resolution of many breathing cycles and a spatial resolution of greater than 5 mm. Blurring of CT images is a necessary step for obtaining the CT-based attenuation map for AC of the PET data, as is scaling of the lower-energy attenuation coefficient in CT images to the attenuation coefficient of 511 keV for AC of PET images (9–11).

Efforts to match the temporal resolution of CT and PET have led to the development of methods that gate the PET data and the CT data, such as 4-dimensional (4D) PET/CT (18–20). The quantification and resolution of PET images can be improved with gating. However, obtaining sufficient data in each gated phase or bin for gated PET normally takes a long time. Gated PET may also require each phase of the gated PET data be matched with the corresponding phase of the CT data for quantification of the PET data. On the basis of our experience with 4D PET/CT studies (18–20), most tumors examined by PET during which patients take a shallow breath do not move in a way that warrants 4D PET. Rather, we have seen many cases of misalignment between HCT and PET data because of the different respiration states of patients during HCT and PET.

In this study, we examined 100 consecutive PET/CT studies for instances of misalignment between HCT and PET. We used the axial extent of the white band or photopenic region at the diaphragm level in the PET images for the measurement of misalignment between the CT and the PET data. The larger the axial extent was, the larger the misalignment was. The HCT data were acquired while the patient was holding a breath at midexpiration, during which CT acquired the data of the thorax.

We also proposed a new method for AC of the PET data; this method uses respiration-averaged CT (ACT) data ob-

tained from multislice 4D CT (21–24) of the thorax. The advantage of using ACT is matching of the temporal resolutions of the CT and the PET data. The ACT data were obtained by averaging the 10 phases of the 4D CT data sets or by averaging the images from a breathing cycle. We evaluated tumor quantification of PET by using HCT and ACT for 13 tumors in the thoraxes of 8 patients (1 patient with esophageal cancer and 7 patients with lung cancer).

MATERIALS AND METHODS

PET/CT with 4D CT Option

Data were acquired on a PET/CT scanner (Discovery ST; GE Healthcare) with a 4D CT option. The CT component of this scanner has a 50-cm transaxial field of view (FOV) and can acquire 8 slices per x-ray tube rotation. The CT slice thickness can range from 1.25 to 10 mm. The x-ray tube current can be varied between 10 and 440 mA, and the tube voltage setting can be 80, 100, 120, or 140 kV (peak). The fastest gantry rotation cycle is 0.5 s, and the maximum helical scan time is 120 s.

The PET component of the Discovery ST scanner is composed of 24 rings of bismuth germanate detectors. The dimensions of each detector element are 6.3, 6.3, and 30 mm in the tangential, axial, and radial directions, respectively. The scanner has a transaxial FOV of 70 cm and an axial FOV of 15.7 cm. The scanner also is capable of acquiring data in 2-dimensional and 3-dimensional modes by retraction of tungsten septa (54 mm long and 0.8 mm thick) from the FOV. The performance of this scanner has been characterized by Mawlawi et al. (25).

A real-time position management optical system (Varian Medical Systems) was mounted at the end of the imaging table to record the respiratory waveform of the patient for synchronization with the data collection for 4D CT (22). The scan times for 20 cm of coverage and 5 s of cine duration are about 1 min with 8-slice CT and 2 min with 4-slice CT (22). The cine 4D CT scanner is commercially available from GE Healthcare.

Protocol and Data Processing

We examined 100 consecutive patient studies for instances of misalignment between HCT and PET with a protocol used in the Department of Nuclear Medicine at The University of Texas M.D. Anderson Cancer Center.

A misalignment was reported when a white band occurred in the lower right thorax in the PET data. The measurement was taken at

TABLE 1
Results of Quantification of Same PET Data Attenuation Corrected by HCT and ACT

Parameter	Data												
	1	2		3	4		5				6	7	8
Patient	1	2	3	4	5	6	7	8	9	10	11	12	13
Tumor	1	2	3	4	5	6	7	8	9	10	11	12	13
Location*	LR	LR	LH	UL	UL	LL	LR	LR	LR	RH	DE	RH	UL
Size (cm)	1.8	1.0	2.0	1.5	0.9	1.4	2.2	1.2	1.4	1.0	2.0	1.7	2.3
SUV (HCT)	2.3	2.6	11.8	10.8	3.9	6.8	6.6	4.6	3.4	4.3	1.9	7.7	9.3
SUV (ACT)	3.6	3.1	12.2	13.7	3.7	6.3	8.4	7.5	4.3	7.4	3.8	9.8	10.9
SUV difference (%) [†]	59.0	17.4	3.6	26.9	-4.7	-7.6	27.4	62.1	28.5	70.1	97.4	27.3	17.2

*LR = lower right; LH = left hilar; UL = upper left; LL = lower left; RH = right hilar; DE = distal esophagus.

[†]Tumors 1, 8, 10, and 11 had SUV differences of more than 50%.

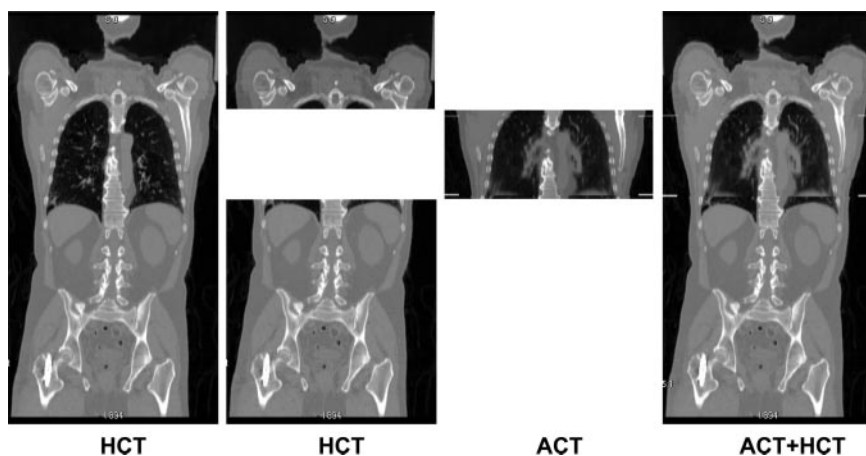


FIGURE 1. Formation of ACT data for PET AC. HCT data are in first panel (left). Some HCT data not overlapping ACT data (third panel) are repeated in second panel. We combined HCT data from second panel and ACT data from third panel to make ACT + HCT data in fourth panel. The main purpose of this fusion was to make ACT + HCT data the same format as HCT for PET AC. All images are coronal. These images were from patient 5 (also shown in Fig. 5).

the peak location of the diaphragm in PET images sliced in the coronal direction. The height of the white band in centimeters was recorded. We also retrospectively analyzed studies of 8 patients (1 with esophageal cancer and 7 with lung cancer) in a comparison of PET quantification with HCT and ACT. These 8 patients (4 men and 4 women) were scanned by 4D CT after their PET/CT studies were performed. Their mean age was 67.6 y, and their ages ranged from 57 to 81 y. Tumors measured less than 2.3 cm. Tumor locations are summarized in Table 1. This study was approved by M.D. Anderson Cancer Center under protocol RCR05-0064. The patients received both PET/CT and 4D CT scans for staging and radiation therapy treatment planning.

All of the patients were injected with 555–740 MBq of ^{18}F -FDG and scanned 1 h after injection. The HCT data were acquired at the following settings: 120 kV, 300 mA, pitch of 1.35:1, collimation of 8×1.25 mm, and gantry rotation cycle of 0.5 s. Patients were instructed to hold their breath at midexpiration during HCT of the thorax. The PET data were acquired for 3 min per 15-cm bed.

We obtained the ACT data by averaging the 10 phases of the 4D CT data for AC of the PET data (18,19,22). The data from 4D CT of the thorax were obtained at the following settings: 120 kV, 50–150 mA, cine duration of 1 breathing cycle plus 1 s, collima-

tion of 8×1.25 mm, and rotation cycle of 0.5 s. The ACT data for the thorax were combined with the HCT data for areas outside the thorax to make up the CT images for AC of the PET data, with an average of 6 bed positions, or a total of 90 cm. We refer to these combined CT data as the ACT data, in the interest of AC of the PET data in the thorax. Figure 1 shows an example of combination of the ACT and the HCT data. Both the ACT and the HCT data were used for AC of the same PET data. The reconstruction of the PET data was performed with 2 iterations of ordered-subset expectation maximization with 30 subsets, a pixel matrix of 128×128 , and an FOV of 50 cm.

RESULTS

Figure 2 shows the alignment results at the lower right diaphragm position between HCT and PET for 100 patient studies. There were 50 patient studies with no misalignment (<1 cm) and 50 patient studies with a misalignment (>1 cm) between HCT and PET; misalignment was identified as a white band in the lower right thorax of the PET data. There were 34 patient studies with a misalignment of more than 2 cm. The largest difference was 6–7 cm, which may

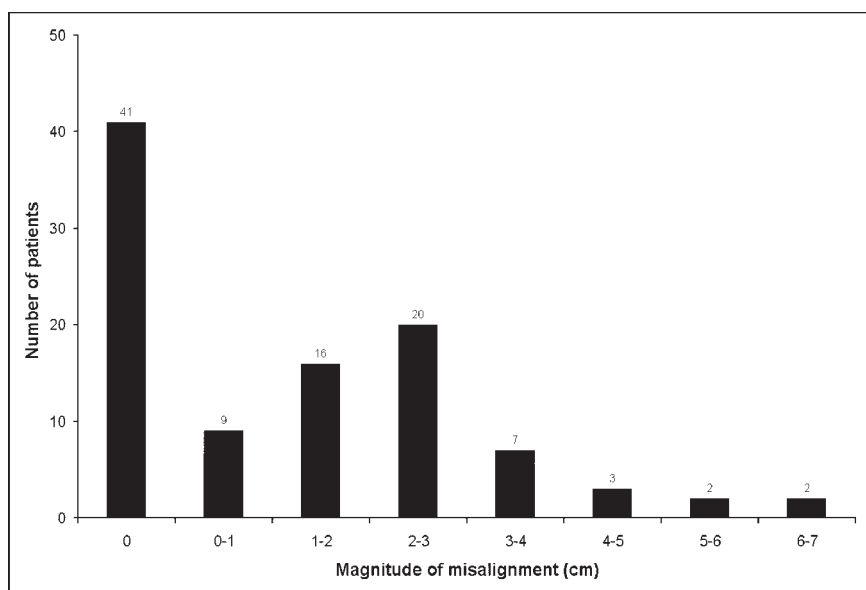


FIGURE 2. Frequency and magnitude of misalignment between PET and HCT of lower right thorax in 100 consecutive PET/CT studies.

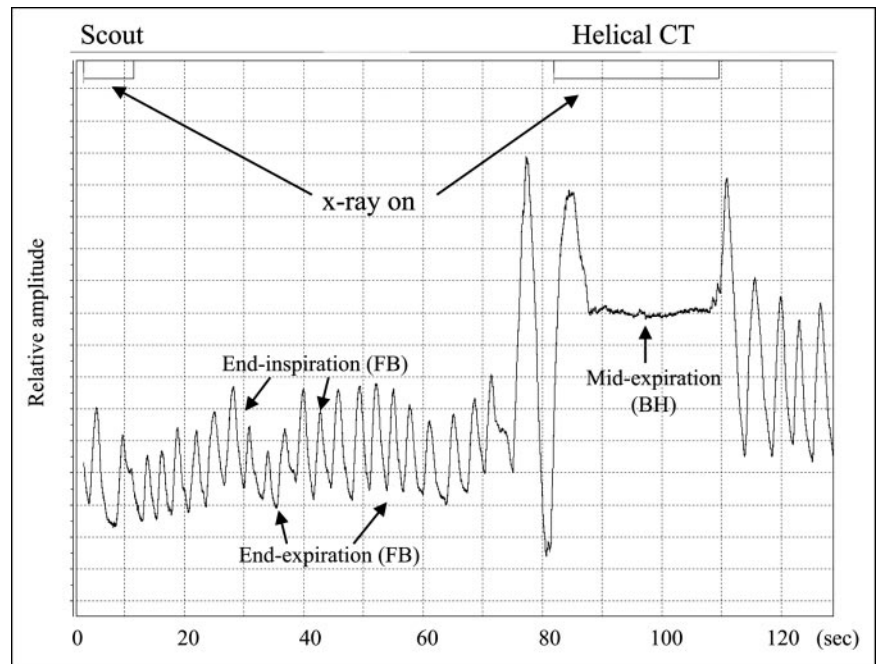


FIGURE 3. Respiratory signal recorded during HCT before PET. Recording was made with strain gauge monitoring respiratory motion around waist at sampling frequency of 1 kHz. Scout scan was taken to survey anatomy; during this scan, patient was breathing freely (FB). After scout scan was taken, patient was instructed to prepare for limited breath-hold (BH) at midexpiration for HCT. It was noted that patient held breath at state different from any breathing state before breath-hold.

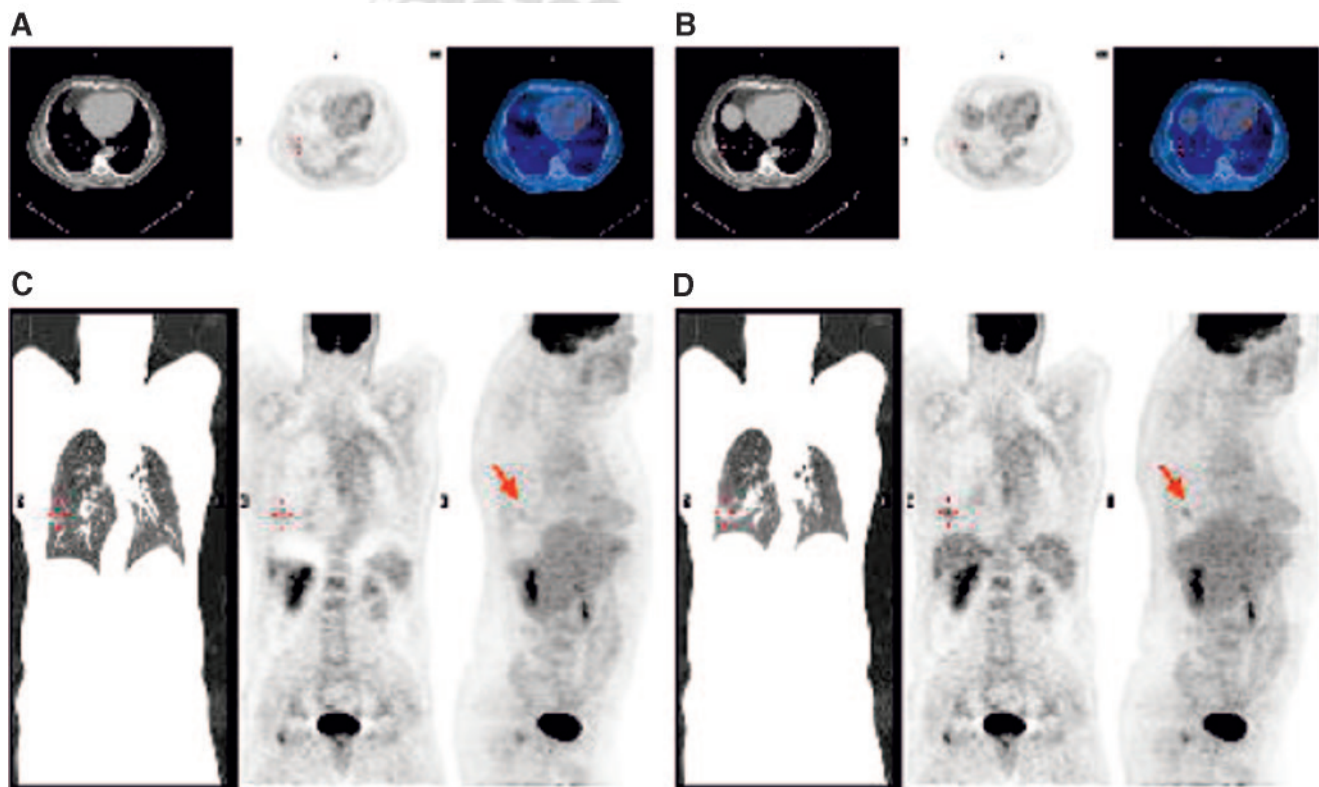


FIGURE 4. (A) Axial HCT and PET data (corrected by HCT) for tumor 1 (patient 1). (B) Corresponding axial ACT and PET data (corrected by ACT). SUV for HCT PET and ACT PET were 2.3 and 3.6, respectively. SUV increased 59.0% from HCT PET to ACT PET. (C) Coronal HCT, HCT PET, and maximum-intensity projection (MIP) of HCT PET data. (D) Coronal ACT, ACT PET, and MIP of ACT PET data. With ACT, there was a significant reduction in breathing artifacts caused by different breathing states during HCT and PET, suggesting that ACT can effectively reduce breathing artifacts and improve quantification of PET data. On each image, crosshair or arrow indicates tumor location. Same tumor can be seen in both ACT and PET data in B but not clear in PET data and not in HCT data in A.

have exceeded the normal range of diaphragm motion during free breathing (26). This finding suggested a potential drawback of limited breath-hold during HCT.

The misalignment is based on the white band in the lower right thorax. The occurrence of a white band indicates a tendency for the patient to hold a deeper breath than for the average PET position in the lower thorax. In this situation, the CT data will indicate a larger area of air in the lungs than the PET data, rendering insufficient AC of the PET data in the lower thorax. If a patient holds a breath near the end of expiration, then it may not be possible to discern any misalignment, because there will not be a white band in the measurements. Therefore, the misalignment found in the 100 patient studies may be larger than what we reported here.

Figure 3 shows an example of a respiratory signal recorded in 1 of the clinical PET/CT studies. The midexpiration state of breath-hold in the HCT data was at an even deeper inspiration than end inspiration in the free-breathing state. This scenario may be the major source of misalignment when the tumor of interest is in the lower thorax.

Table 1 shows the results of AC of the same PET data by HCT when patients held their breath at midexpiration and by ACT when patients took a normal breath. There were 5

tumors from 3 patients with differences in standardized uptake values (SUV) of less than 20% and 4 tumors (tumors 1, 8, 10, and 11) from 3 patients with SUV differences of more than 50%. The tumors with more than a 50% change in SUV came from the patient with esophageal cancer and from 2 of the patients with lung cancer. For these 3 patients, there was a misalignment of 2–4.5 cm in the lower right thorax between HCT and PET. Breathing artifacts or misalignments were significantly reduced in the PET data that were corrected by ACT. Seven of the 8 patients had a lower diaphragm position on HCT than on ACT, suggesting that patients tended to hold a deeper breath during HCT than the average breathing state. Figures 4–6 show images of the HCT, ACT, and PET data corrected with HCT and ACT for tumors of no. 1, 10, and 11, with SUV changes of 59.0%, 70.1%, and 97.4%, respectively.

DISCUSSION

Our study demonstrated the potential misalignment caused by different breathing states during HCT and PET and showed that the use of ACT reduces breathing artifacts and improves tumor quantification. Therefore, the ideal CT

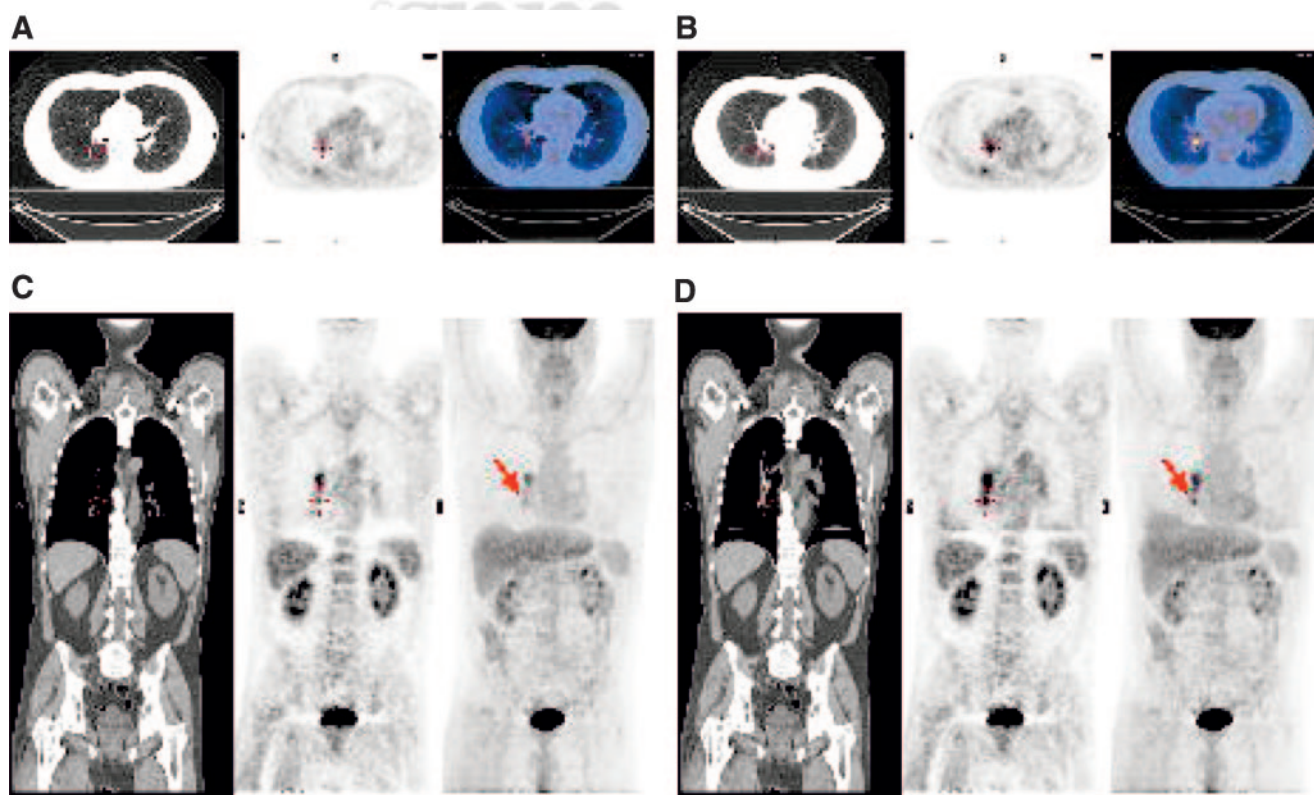


FIGURE 5. (A) Axial HCT and PET data (corrected by HCT) for tumor 10 (patient 5). (B) Corresponding axial ACT and PET data (corrected by ACT). To augment interpretation, both HCT and ACT images are shown with CT level of -700 and window width of $1,000$. SUV for HCT PET and ACT PET were 4.3 and 7.4 , respectively. SUV increased 70.1% from HCT PET to ACT PET. (C) Coronal HCT, HCT PET, and maximum-intensity projection (MIP) of HCT PET data. (D) Coronal ACT, ACT PET, and MIP of ACT PET data. With ACT, there was a significant reduction in breathing artifacts caused by different breathing states during HCT and PET. Note that ACT did not cover whole lung and was still able to correct for breathing artifacts. On each image, crosshair or arrow indicates tumor location.

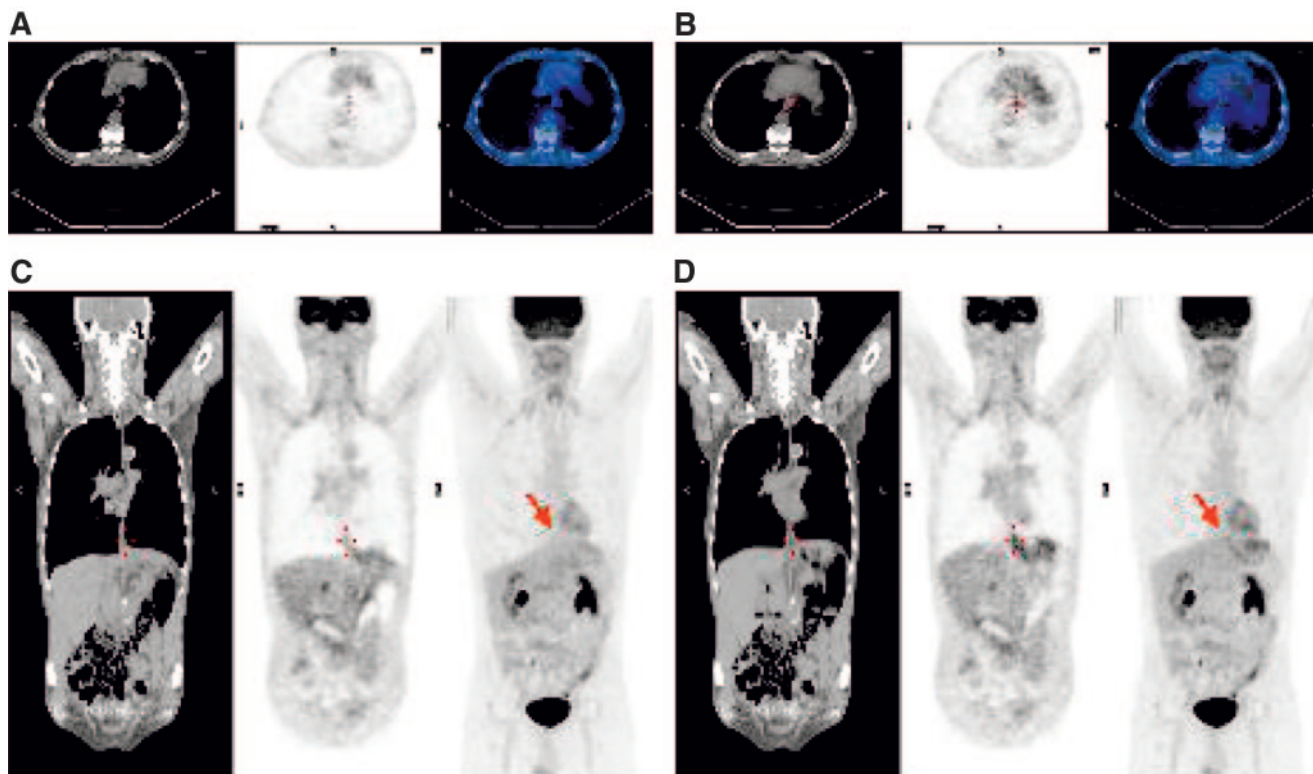


FIGURE 6. (A) Axial HCT and PET data (corrected by HCT) for tumor 11 (patient 6). (B) Corresponding ACT and PET data (corrected by ACT). SUV for HCT PET and ACT PET were 1.9 and 3.8, respectively. SUV increased 97.4% from HCT PET to ACT PET. (C) Coronal HCT, HCT PET, and maximum-intensity projection (MIP) of HCT PET data. (D) Coronal ACT, ACT PET, and MIP of ACT PET data. With ACT, there was a significant reduction in breathing artifacts caused by different breathing states during HCT and PET. On each image, crosshair or arrow indicates tumor location.

for AC of the PET data will be a combination of HCT covering the anatomy above and below the thorax and ACT covering the anatomy in the thorax, as suggested in Figure 1. The current dose used in 4D CT for a cine duration of 5 s is between 23 and 70 mGy for 50–150 mA at a gantry rotation cycle of 0.5 s. This dose is not a critical issue in radiation therapy planning. However, for a routine diagnostic procedure, this dose is considerably high. We are currently investigating ways to minimize the radiation dose of 4D CT and to achieve the same effects as those seen with ACT in this study.

CONCLUSION

We analyzed the frequency and magnitude of misalignment between the HCT and the PET data in 100 consecutive PET/CT studies with a limited breath-hold during HCT. Fifty studies showed a misalignment between HCT and PET, and 34 studies showed a misalignment of more than 2 cm, suggesting that efforts should be made to reduce the misalignment. We have proposed the use of ACT for AC of the PET data for the thorax to reduce the misalignment attributable to the different breathing states during HCT and PET and to improve the quantification of the PET data. The main advantage of ACT over HCT is that the temporal

resolution of 1 breathing cycle in ACT is similar to that of many repeat breathing cycles in PET.

In a study of 13 tumors in 8 patients, we found 4 tumors in 3 patients with an SUV change of more than 50%, and these 3 patients had a misalignment of 2–4.5 cm. Breathing artifacts, shown as a white band in the lower thorax of PET images, were significantly reduced by ACT. The results demonstrate that a significant change in SUV could be attributable to the mismatch between breathing states during HCT and PET and suggest a better match of ACT and PET than of HCT and PET and more accurate PET quantification in the thorax by ACT than by HCT.

ACKNOWLEDGMENT

This work was supported in part by a start-up fund from The University of Texas M.D. Anderson Cancer Center.

REFERENCES

1. Beyer T, Townsend DW, Brun T, et al. A combined PET/CT scanner for clinical oncology. *J Nucl Med.* 2000;41:1369–1379.
2. Kluetz PG, Meltzer CC, Villemagne V, et al. Combined PET/CT imaging in oncology: impact on patient management. *Clin Positron Imaging.* 2000;3:223–230.
3. Bar-Shalom R, Yefremov N, Guralnik L, et al. Clinical performance of PET/CT in evaluation of cancer: additional value for diagnostic imaging and patient management. *J Nucl Med.* 2003;44:1200–1209.

4. Hany TF, Steinert HC, Goerres GW, Buck A, von Schulthess GK. PET diagnostic accuracy: improvement with in-line PET-CT system: initial results. *Radiology*. 2002;225:575–581.
5. Charron M, Beyer T, Bohnen NN, et al. Image analysis in patients with cancer studied with a combined PET and CT scanner. *Clin Nucl Med*. 2000;25:905–910.
6. Lardinois D, Weder W, Hany TF, et al. Staging of non-small-cell-lung cancer with integrated positron-emission tomography and computed tomography. *N Engl J Med*. 2003;348:2500–2507.
7. Schoder H, Erdi YE, Larson SM, Yeung HWD. PET/CT: a new imaging technology in nuclear medicine. *Eur J Nucl Med Mol Imaging*. 2003;30:1419–1437.
8. Townsend DW, Carney JPI, Yap JT, Hall NC. PET/CT today and tomorrow. *J Nucl Med*. 2004;45(suppl):4S–14S.
9. Kinahan PE, Townsend DW, Beyer T, Sashin D. Attenuation correction for a combined 3D PET/CT scanner. *Med Phys*. 1998;25:2046–2053.
10. Burger C, Goerres GW, Schoenes S, Buck A, Lonn AHR, von Schulthess GK. PET attenuation coefficients from CT images: experimental evaluation of the transformation of CT into PET 511-keV attenuation coefficients. *Eur J Nucl Med*. 2002;29:922–927.
11. Nakamoto Y, Osman M, Cohade C, et al. PET/CT: comparison of quantitative tracer uptake between germanium and CT transmission attenuation-corrected images. *J Nucl Med*. 2002;43:1137–1143.
12. Beyer T, Antoch G, Mueller S, et al. Acquisition protocol considerations for combined PET/CT imaging. *J Nucl Med*. 2004;45(suppl):25S–35S.
13. Osman MM, Cohade C, Nakamoto Y, Wahl RL. Respiratory motion artifacts on PET emission images obtained using CT attenuation correction on PET-CT. *Eur J Nucl Med Mol Imaging*. 2003;30:603–606.
14. Osman MM, Cohade C, Nakamoto Y, Mashall LT, Leal JP, Wahl RL. Clinically significant inaccurate localization of lesions with PET/CT: frequency in 300 patients. *J Nucl Med*. 2003;44:240–243.
15. Goerres GW, Kamel E, Seifert B, et al. Accuracy of image coregistration of pulmonary lesions in patients with non-small cell lung cancer using an integrated PET/CT system. *J Nucl Med*. 2002;43:1469–1475.
16. Goerres GW, Kamel E, Heidelberg TN, Schwitter MR, Burger C, von Schulthess GK. PET-CT image co-registration in the thorax: influence of respiration. *Eur J Nucl Med Mol Imaging*. 2002;29:351–360.
17. Beyer T, Antoch G, Blodgett T, Freudenberg LF, Akhurst T, Mueller S. Dual-modality PET/CT imaging: the effect of respiratory motion on combined image quality in clinical oncology. *Eur J Nucl Med Mol Imaging*. 2003;30:588–596.
18. Nehmeh SA, Erdi YE, Pan T, et al. Quantitation of respiratory motion during 4D-PET/CT acquisition. *Med Phys*. 2004;31:1333–1338.
19. Erdi YE, Nehmeh SA, Pan T, et al. The CT motion quantitation of lung lesions and its impact on PET-measured standardized uptake values. *J Nucl Med*. 2004;45:1287–1292.
20. Nehmeh SA, Erdi YE, Pan T, et al. Four-dimensional (4D) PET/CT imaging of the thorax. *Med Phys*. 2004;31:3179–3186.
21. Low DA, Nystrom M, Kalinin E, et al. A method for the reconstruction of four-dimensional synchronized CT scans acquired during free breathing. *Med Phys*. 2003;30:1254–1264.
22. Pan T, Lee TY, Rietzel E, Chen GTY. 4D-CT imaging of a volume influenced by respiratory motion on multi-slice CT. *Med Phys*. 2004;31:333–340.
23. Keall PJ, Starkschall G, Shukla H, et al. Acquiring 4D thoracic CT scans using a multislice helical method. *Phys Med Biol*. 2004;49:2053–2067.
24. Pan T. Comparison of helical and cine acquisitions for 4D-CT imaging with multi-slice CT. *Med Phys*. 2005;32:627–634.
25. Mawlawi O, Podoloff DA, Kohlmyer S, et al. Performance characteristics of a newly developed PET/CT scanner using NEMA standards in 2D and 3D modes. *J Nucl Med*. 2004;45:1734–1742.
26. Seppenwoolde Y, Shirato H, Kitamura K, et al. Precise and real-time measurement of 3D tumor motion in lung due to breathing and heartbeat, measured during radiotherapy. *Int J Radiat Oncol Biol Phys*. 2002;53:822–834.





The Journal of
NUCLEAR MEDICINE

Attenuation Correction of PET Images with Respiration-Averaged CT Images in PET/CT

Tinsu Pan, Osama Mawlawi, Sadek A. Nehmeh, Yusuf E. Erdi, Dershan Luo, Hui H. Liu, Richard Castillo, Radhe Mohan, Zhongxing Liao and H.A. Macapinlac

J Nucl Med. 2005;46:1481-1487.

This article and updated information are available at:
<http://jnm.snmjournals.org/content/46/9/1481>

Information about reproducing figures, tables, or other portions of this article can be found online at:
<http://jnm.snmjournals.org/site/misc/permission.xhtml>

Information about subscriptions to JNM can be found at:
<http://jnm.snmjournals.org/site/subscriptions/online.xhtml>

The Journal of Nuclear Medicine is published monthly.
SNMMI | Society of Nuclear Medicine and Molecular Imaging
1850 Samuel Morse Drive, Reston, VA 20190.
(Print ISSN: 0161-5505, Online ISSN: 2159-662X)

© Copyright 2005 SNMMI; all rights reserved.